ELSEVIER

Shape of ammonium chloride dendrite tips at small supersaturation

Andrew Dougherty*, Mayank Lahiri

Department of Physics, Lafayette College, Easton, PA 18042, USA

Abstract

We report detailed shape measurements of the tips of three-dimensional NH_4Cl dendrites grown from supersaturated aqueous solution. For growth at small supersaturation, we compare two models for the tip shape: parabolic with a fourth-order correction and a power law. Neither is ideal, but the fourth-order fit appears to provide the most robust description of both the tip shape and position for this material. For that fit, the magnitude of the fourth-order coefficient is about half of the theoretically expected value.
© 2004 Elsevier B.V. All rights reserved.

1. Introduction

Dendrites are a commonly observed microstructural form resulting from the diffusion-limited solidification of non-faceting materials, and they continue to be interesting for both practical and fundamental reasons. Practically, an improved understanding of dendritic microstructures may

enhance the ability to predict and control material properties. Fundamentally, they are an intriguing example of pattern formation under non-linear and non-equilibrium conditions [1–4].

Two of the most basic experimental characterizations of a growing dendrite are the tip size and growth speed. Although there is already considerable data available, recent advances in both theory and experimental technique have made more precise comparisons between them possible. Some comparisons have already been made for some pure materials [5,6], but it is important that they also be made for as broad a range of systems as is

---
*Corresponding author. Tel.: +16103305212; fax: +16103305714.

E-mail address: doughera@lafayette.edu (A. Dougherty).

URL: http://www.lafayette.edu/%7Edoughera/.

reasonable, in order to clarify the roles of various effects such as solution vs. thermal growth, and different values of crystalline anisotropy.

In the absence of surface tension, one solution to the diffusive growth problem is a parabolic dendrite with radius of curvature ρ propagating at constant speed v. However, the presence of surface tension, and the instabilities that lead to side-branching, complicate the problem considerably. Indeed, even the most basic issues about the precise tip shape [5–10] and whether a dendrite actually grows with a constant velocity [11–14] are still areas of active research.

Addressing those issues requires unambiguous ways to identify both the tip size and position. In this paper, we consider two different models for the dendrite tip shape and evaluate their use to characterize the growth of NH$_4$Cl dendrites at small supersaturations. A similar exploration of different tip shape models for dendrites resulting from phase-field simulations was reported by Karma et al. [8], but it is important to investigate how well the different models work for different materials under actual observation conditions.

2. Background

A typical dendrite of NH$_4$Cl grown in this study is shown in Fig. 1. Since NH$_4$Cl has cubic symmetry, four sets of sidebranches grow approximately perpendicular to the main dendrite stem. In Fig. 1, two sets of sidebranches are visible in the plane of the image; two additional branches are growing perpendicular to the plane of the image.
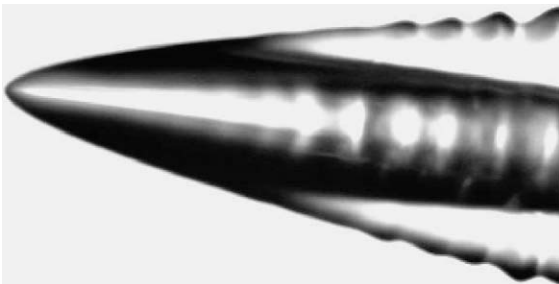

Fig. 1. Dendrite of NH$_4$Cl. The picture is approximately 400 μm across.
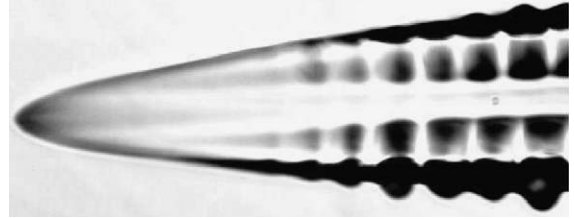

Fig. 2. Dendrite of NH$_4$Cl with $\phi \approx 45°$. The scale is the same as in Fig 1.

The coordinate system used in this work is defined as follows. The main dendrite stem is used to define the z-axis. The growth direction is taken as the negative-z direction, so the solid crystal lies along the positive z-axis. The x-axis is defined as the direction in the plane of the image perpendicular to z. Lastly, ϕ is defined to be the rotation angle of the crystal around the z-axis. A dendrite with $\phi \approx 45°$ is shown in Fig. 2.

2.1. Parabolic fit with fourth-order correction

For diffusion-controlled growth in the absence of surface tension, the Ivantsov solution is a paraboloid of revolution of radius ρ growing at speed v. Once anisotropic surface tension is included, microscopic solvability [3,15] predicts both the tip size ρ and speed v depend on the crystalline anisotropy ε_4. For a fourfold-symmetric crystal such as NH$_4$Cl, that anisotropy can be expressed in spherical coordinates as [9]

$$\gamma(\Theta, \Phi)/\gamma_0 = 1 + \varepsilon_4[4\cos^4\Theta + (3 + \cos 4\Phi)\sin^4\Theta], \qquad (1)$$

where γ is the surface free energy, and Θ and Φ are the usual spherical angles.

Although the presence of anisotropic surface tension is critical for the development of the dendritic structure, the overall magnitude of the surface tension is small, so the deviations of the tip shape from parabolic might be expected to be rather small as well. Many experiments, including the landmark experiments of Glicksman and Huang [16], confirm that a parabola is indeed a reasonably good approximation to the tip shape.

Experiments on NH_4Br also showed that a parabola is a reasonably good approximation, at least relatively close to the tip [17].

In the limit of small fourfold-anisotropy, Amar and Brener [18] found that the lowest-order correction to the parabolic shape is a fourth-order term proportional to $\cos 4\phi$, where ϕ is the rotation angle around the z-axis. Thus, at least close to the tip, the tip shape could be reasonably well described by

$$z = z_{tip} + \frac{(x - x_{tip})^2}{2\rho} - A_4 \cos 4\phi \frac{(x - x_{tip})^4}{\rho^3}, \quad (2)$$

where (x_{tip}, z_{tip}) is the location of the tip, ρ is the radius of curvature at the tip, and $A_4 = \frac{1}{96}$, independent of anisotropy strength [19]. Using a somewhat different approach, McFadden et al. [9] found that, to second order in ε_4, $A_4 = \varepsilon_4 + 12\varepsilon_4^2$, at least very close to the tip. Using an estimate of $\varepsilon_4 \approx 0.016$ (the value reported for NH_4Br [17]) this corresponds to $A_4 \approx 0.019$.

Tip shapes consistent with this model were found by LaCombe and coworkers [5,11]. They studied succinonitrile dendrite tips under a variety of three-dimensional crystal orientations, evaluated both second- and fourth-order polynomial fits, and concluded that the fourth-order fit worked significantly better [5,11].

2.2. Power law

Further back from the tip, the crystalline anisotropy tends to concentrate material into four "fins" such that the shape is no longer well described by Eq. (2). The width of the fins is predicted [20] to scale as $(z - z_{tip})^{3/5}$. Scaling consistent with this prediction was observed in the average shapes of NH_4Cl and pivalic acid dendrites grown from solution [21,22].

Although this power-law scaling was originally proposed to describe the shape of the crystal in the region *behind* the tip, Bisang and Bilgram found that for xenon dendrites with $\phi \approx 0$, this power law was a good fit even quite close to the tip [10,23]. Hence, the power law offers another way to characterize the tip size and location.

In this model, we describe the tip shape by

$$z = z_{tip} + \frac{|x - x_{tip}|^{5/3}}{(2\rho)^{2/3}}, \quad (3)$$

where we have included the factor of 2 by analogy with Eq. (2). The parameter ρ still sets a length scale for the dendritic structure, but the curvature at the tip is no longer defined.

2.3. Experimental considerations and model limitations

Each of these models has different limitations. From the theoretical perspective, the fourth-order fit is only appropriate very close to the tip, well before sidebranches become significant. Hence, in order to avoid contamination from sidebranches, only data with $(z - z_{tip}) < z_{max}$ should be used in the fit. Since sidebranching activity is detectable even close to the tip (at least for NH_4Br dendrites [24]), z_{max} should not be made too large. On the other hand, z_{max} should not be made too small since the region around the tip contains the sharpest curvatures and the largest concentration gradients, and hence it is subjected to the maximum optical distortions [5,17]. Considering both issues, Dougherty and Gollub [17] suggested $z_{max} = 3\rho$ as a compromise for parabolic fits.

In contrast, the power-law fit is only appropriate further behind the tip, so its usefulness for describing the tip size and position must be explicitly tested. However, since it is not necessarily constrained to as small z_{max}, the fit can include data points less contaminated by optical distortions near the tip. On balance, for xenon dendrites with $\phi \approx 0$, Bisang and Bilgram found that this power law provided a reasonable fit.

Both models are potentially sensitive to the choice of z_{max} used in the fitting procedure, though such dependence ought to be minimal if an appropriate fitting function is used. Singer and Bilgram discuss a procedure to determine ρ from polynomial fits in a way that is somewhat less model dependent [25], but that approach did not offer any significant advantage for this system.

Thus, both the fourth-order and the power-law fit provide reasonable fits, at least in some cases,

but a direct comparison of the two models for the same material is required for an accurate assessment.

3. Experiments

The experiments were performed with aqueous solutions of ammonium chloride with approximately 36% NH_4Cl by weight. The saturation temperature was approximately 65 °C. The solution was placed in a $45 \times 12.5 \times 2\,mm^3$ glass cell and sealed with a teflon stopper. The cell was mounted in a massive temperature-controlled copper block surrounded by an insulated temperature-controlled aluminum block, and placed on the stage of an Olympus BH-2 microscope. The entire microscope was enclosed in an insulating box.

The temperature of the outer aluminum block was controlled by an Omega CN-9000 controller to approximately ±1 °C. The temperature of the inner copper block was controlled directly by computer. A thermistor in the block was connected via a Kiethley 2000 digital multi-meter to the computer, where the resistance was converted to temperature. The computer then controlled the heater power supply using a software version of a proportional-integral controller. This allowed very flexible control over not just the temperature, but also over any changes in the temperature, such as those used to initiate growth. The temperature of the sample was stable to within approximately $±5 \times 10^{-4}$ °C.

A charged-coupled device (CCD) camera was attached to the microscope and images were acquired directly into the computer with a Data Translation DT3155 frame grabber with a resolution of 640×480 pixels. The ultimate resolution of the images was $0.63 \pm 0.01\,\mu m/pixel$. As a backup, images were also recorded onto video tape for later use.

To obtain crystals, the solution was heated to dissolve all the NH_4Cl, stirred to eliminate concentration gradients, and then cooled to initiate growth. Typically, many crystals would nucleate. An automated process was set up to acquire images and then slowly adjust the temperature until all but the largest crystal had dissolved.

This isolated crystal was allowed to stabilize for several days. The temperature was then reduced by 0.77 °C and the crystal was allowed to grow. The crystal was initially approximately spherical, but due to the cubic symmetry of NH_4Cl, six dendrite tips would begin to grow. The tip with the most favorable orientation was followed, and images were recorded at regular intervals.

The interface position was determined in the same manner as in Ref. [17]. The intensity in the image was measured on a line perpendicular to the interface. Over the range of a few pixels, the intensity changes rapidly from bright to dark. Deeper inside the crystal, the intensity begins to rise again. (This corresponds to the brighter areas inside the crystal in Fig. 1.) In the bright-to-dark transition region, we fit a straight line to the intensity profile. We define the interface as the location where the fitted intensity is the average of the high value outside the crystal and the low value just inside the crystal.

This fitting procedure interpolates intensity values and allows a reproducible measure of the interface to better than one pixel resolution. It is also insensitive to absolute light intensity levels, to variations in intensity across a single image, and to variations in intensity *inside* the crystal well away from the interface. For the simple shapes considered here, this method is more robust and requires less manual intervention than a more general contour-extraction method, such as the one described by Singer and Bilgram for more complex crystal shapes [26].

This method works best if the image is scanned along a line perpendicular to the interface. Since the position and orientation of the interface are originally unknown, an iterative procedure is used until subsequent iterations make no significant change to the fit. Specifically, we start with an initial estimate of the size, location, and orientation of the tip, and use that to scan the image to obtain a list of interface positions up to a distance z_{max} back from the tip (where z_{max} is some multiple of ρ). We next rotate the data by an angle θ in the x–z plane and perform a non-linear regression on Eqs. (2) or (3) to determine the best fit values for

x_{tip}, z_{tip}, ρ, and A_4 (if applicable), and the corresponding χ^2 value. We then repeat with different θ values and minimize χ^2 using Brent's algorithm [27]. This completes one iteration of the fitting procedure. We use this result to rescan the image along lines perpendicular to the interface to obtain a better estimate of the interface location and begin the next iteration. The procedure usually converges fairly rapidly. Even for a relatively poor initial estimate, it typically takes fewer than 20 iterations.

There are some subtleties to the procedure worth noting. First, for a typical crystal in this work such as in Fig. 1, only about 120 data points are involved in the fit for $z_{max} = 6\rho$. For the fourth-order fit with five free parameters, there are often a number of closely spaced local minima in the χ^2 surface, with tip positions and radii varying by a few hundredths of a micrometer. If the iterative procedure enters a limit cycle instead of settling down to a single final value, we select the element from that limit cycle with the minimum χ^2. Second, we have no way to control or precisely measure the orientation angle ϕ of the crystals in our system. In Ref. [5], the authors were able to determine ϕ by viewing the crystal along two perpendicular directions, but the thin horizontal cell used in this work only offers one optical axis.

4. Results

The best estimates of ρ as a function of z_{max}/ρ for the crystal in Fig. 1 are shown in Fig. 3. We have included results for the fourth-order and power-law fits as well as for a simple parabola for comparison. The corresponding χ^2 values are shown in Fig. 4.

None of the fits is robust very close to the tip, indicating that the actual tip shape is not well described by any of the candidate functions. The parabolic fit also gets rapidly worse for z_{max} greater than about 5ρ. The fourth-order fit appears to have a plateau between roughly 5 and 8ρ, but ρ gradually increases with z_{max}, and the χ^2 value rapidly increases for $z_{max} > 10\rho$. By contrast, the power law fit gives relatively stable values at large z_{max} for both ρ and χ^2.
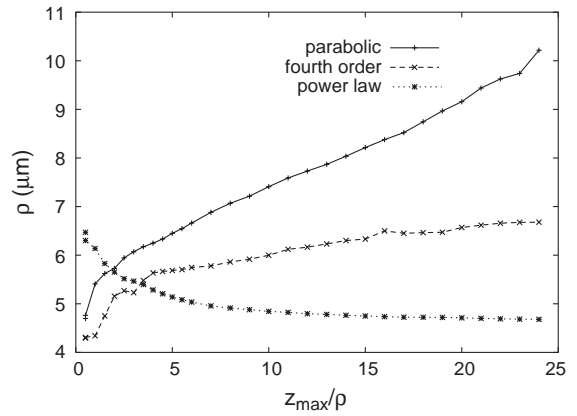

Fig. 3. Best fit value of ρ as a function of z_{max}/ρ for the crystal shown in Fig. 1. The curves are for a parabolic fit (+), a fourth-order fit (×), and a power-law fit (∗).
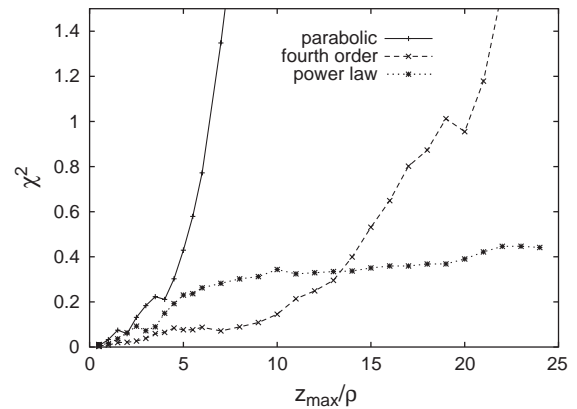

Fig. 4. Values of χ^2 for the best fit as a function of z_{max}/ρ for the crystal shown in Fig. 1. The curves are for a parabolic fit (+), a fourth-order fit (×), and a power-law fit (∗).

A second important consideration is the degree to which each fit accurately describes the tip location. This is illustrated in Fig. 5, which shows x_{tip} for each fit. Here again, the fourth-order fit is slightly more robust than the power-law.

Finally, Fig. 6 shows the original data along with each of the three model fits superposed for $z_{max} = 6\rho$. Of the three fits, the fourth-order does the best job of capturing both the tip location and shape.
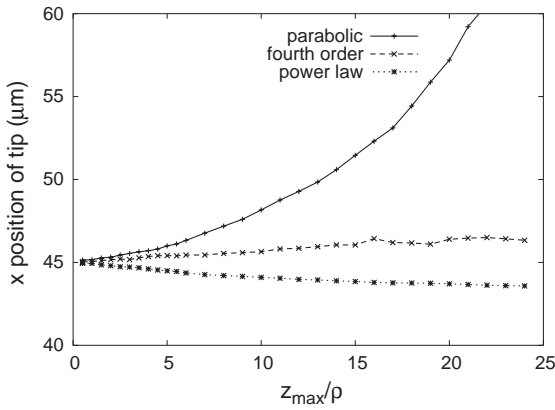
Fig. 5. Best-fit values for the *x*-position of the tip as a function of z_{max}/ρ for the crystal shown in Fig. 1. Symbols are as in the previous figures.
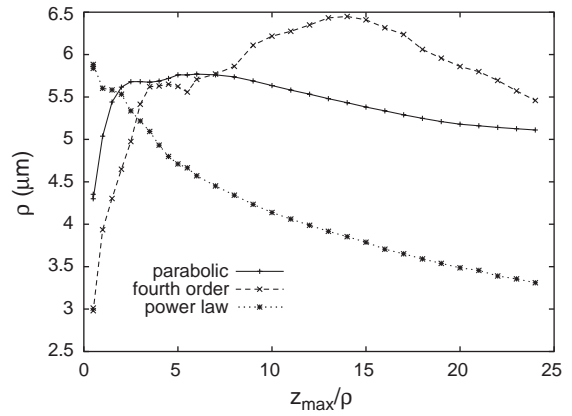

Fig. 7. Best fit value of ρ as a function of z_{max}/ρ for the crystal shown in Fig. 2. The curves are for a parabolic fit (+), a fourth-order fit (×), and a power-law fit (∗).
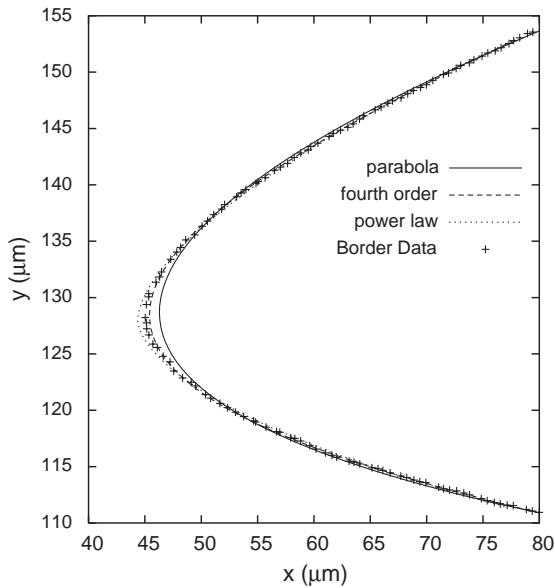

Fig. 6. Best-fit parabolic (solid), fourth-order (dashed), and power-law (dotted) curves for $z_{max} = 6\rho$, along with the original border (+) for the crystal shown in Fig. 1. Near the tip, the parabolic fit is too far to the right, while the power-law fit is too far to the left. The fourth-order fit matches the tip region fairly well.
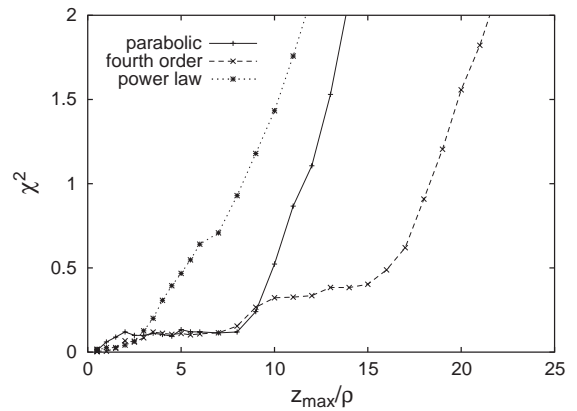

Fig. 8. Values of χ^2 for the best fit as a function of z_{max}/ρ for the crystal shown in Fig. 2. The curves are for a parabolic fit (+), a fourth-order fit (×), and a power-law fit (∗).

For the value of $z_{max} = 6\rho$, we find $A_4 = 0.004 \pm 0.001$, which is similar to that measured by LaCombe et al. for succinonitrile [5,11], and to that obtained in the simulations by Karma et al. [8]. This value for A_4 is less than the value of $\frac{1}{96}$ predicted by Brener and Mel'nikov [19], and also significantly less than the value of 0.019 estimated by McFadden et al. [9]. It is worth noting, however, that these predictions are only intended to be valid close to the tip, where our fit is not robust.

The results are slightly different for the crystal shown in Fig. 2, which has $\phi \approx 45°$. The best estimates of ρ as a function of z_{max}/ρ for the three fits are shown in Fig. 7, and the corresponding χ^2 values are shown in Fig. 8.

Both the parabolic and fourth order models fit reasonably well for z_{max} between roughly 5 and 8ρ. Indeed within that range, for the entire run from which Fig. 2 was taken, the value for A_4 is 0.0007 ± 0.0009, consistent with zero. In contrast, the power law is a poor fit.

One significant problem with this measurement is that the image in Fig. 2 is a projection of the true three-dimensional shape. This is discussed in Refs. [5,11] and in considerably more detail in Ref. [8], but, in general, our findings are consistent with those of LaCombe et al. [5,11].

5. Conclusions

We have considered two different models for the tip shape: parabolic with a fourth-order correction, and power law. For crystals oriented such that $\phi \approx 0$, both give reasonable fits, though the fourth-order fit is slightly better. For rotated crystals, such as those in Fig. 2, however, the fourth-order fit is significantly more robust.

For the crystal in Fig. 1, the coefficient of the fourth-order term is $A_4 = 0.004 \pm 0.001$, significantly less than the theoretically expected value. These findings are consistent with those of LaCombe et al. [5,11] for succinonitrile dendrites.

By contrast, the power-law fit was reasonably robust for $\phi \approx 0$, in agreement with the results of Bisang and Bilgram [10,23] for xenon dendrites, but it did not work as well for crystals with $\phi \approx 45°$. (One important feature of the experiments in Refs. [10,23] was the ability to control the viewing angle and hence ϕ.)

One other problem with the power-law fit is that it does not accurately describe the crystal shape near the tip. Accordingly, it may be more difficult to use a power law fit to look for the onset of sidebranching or possible tip oscillations.

On balance, if the tip can be imaged with reasonably high precision, then the fourth-order fit is probably better, since it works well for all ϕ,

closely matches the tip shape and position, and is readily compared with theoretical predictions. If, however, the tip region cannot be resolved well, then the power law may yield the best estimate of the tip size for crystals with $\phi \approx 0$, since it can incorporate data much further back from the tip.

Two remaining issues may be relevant for all of the models. First, the extent to which optical distortions near the tip affect the results has not been addressed. Specifically, since both the concentration gradients and the interfacial curvature are largest near the tip, the data closest to the tip are the least reliable [5,17]. Second, the extent to which all of these fits are contaminated by early sidebranches needs to be investigated. This may be especially important in characterizing the emergence of sidebranches as well as in studies of possible tip oscillations.

References

[1] W. Boettinger, S. Coriell, A. Greer, A. Karma, W. Kurz, M. Rappaz, R. Trivedi, Acta Mater. 48 (2000) 43.
[2] M.E. Glicksman, S.P. March, in: D.J.T. Hurle (Ed.), Handbook of Crystal Growth, Elsevier Science, Amsterdam, 1993, p. 1081.
[3] D.A. Kessler, J. Koplik, H. Levine, Adv. Phys. 37 (1988) 255.
[4] J. Langer, Rev. Mod. Phys. 52 (1980) 1.
[5] J.C. LaCombe, M.B. Koss, V.E. Fradkov, M.E. Glicksman, Phys. Rev. E 52 (1995) 2778.
[6] U. Bisang, J. Bilgram, J. Crystal Growth 166 (1996) 212.
[7] U. Bisang, J. Bilgram, J. Crystal Growth 166 (1996) 207.
[8] A. Karma, Y. Lee, M. Plapp, Phys. Rev. E 61 (2000) 3996.
[9] G.B. McFadden, S.R. Coriell, R.F. Sekerka, Acta Mater. 48 (2000) 3177.
[10] U. Bisang, J. Bilgram, Phys. Rev. E 54 (1996) 5309.
[11] M. Koss, J. Lacombe, L. Tennenhouse, M. Glicksman, E. Winsa, Metall. Mater. Trans. A 30 (1999) 3177.
[12] J. Lacombe, M. Koss, D. Corrigan, A. Lupulescu, L. Tennenhouse, M. Glicksman, J. Crystal Growth 206 (1999) 331.
[13] J. Lacombe, M. Koss, M. Glicksman, Phys. Rev. Lett. 83 (1999) 2997.
[14] J.C. LaCombe, M. Koss, J.E. Frei, C. Giummarra, A.O. Lupulescu, M.E. Glicksman, Phys. Rev. E 65 (2002) 031604.
[15] D.A. Kessler, H. Levine, Acta Metall. 36 (1988) 2693.
[16] M.E. Glicksman, S.-C. Huang, Acta Metall. 29 (1981) 701.
[17] A. Dougherty, J.P. Gollub, Phys. Rev. A 38 (1988) 3043.
[18] M.B. Amar, E. Brener, Phys. Rev. Lett. 71 (1993) 589.
[19] E. Brener, V.I. Mel'nikov, JETP 80 (1995) 341.

[20] E. Brener, Phys. Rev. Lett. 71 (1993) 3653.
[21] A. Dougherty, R. Chen, Phys. Rev. A 46 (1992) R4508.
[22] A. Dougherty, A. Gunawardana, Phys. Rev. E 50 (1994) 1349.
[23] U. Bisang, J.H. Bilgram, Phys. Rev. Lett. 75 (1995) 3898.
[24] A. Dougherty, P.D. Kaplan, J.P. Gollub, Phys. Rev. Lett. 58 (1987) 1652.
[25] H.M. Singer, J. Bilgram, Phys. Rev. E 69 (2004) 032601.
[26] H.M. Singer, J. Bilgram, J. Crystal Growth 261 (2004) 122.
[27] W.H. Press, S.A. Teukolsky, W.T. Vetterling, B.P. Flannery, Numerical Recipes in C, Cambridge University Press, Cambridge, 1992.